Case Studies in Construction Materials 21 (2024) e03538

Contents lists available at ScienceDirect

Case Studies in Construction Materials

journal homepage: www.elsevier.com/locate/cscm

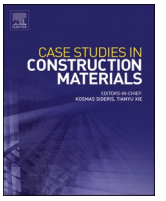

Sustainable stabilization of waste foundry sands in alkali activated glass-based matrices

Francesco Cammelli [a,b], Giulia Tameni [a], Enrico Bernardo [a,b,*]

[a] Department of Industrial Engineering, University of Padova, Padova, Italy
[b] RU INSTM, University of Padova, Italy

ARTICLE INFO

Keywords:
Alkali activation
Up-cycling
Boro-alumino-silicate glass waste
Foundry sands
Leaching test
Compressive test

ABSTRACT

Since cements and concrete are highly energy-demanding, sustainable construction materials represent a crucial aspect in mitigating environmental pollution. The study proposes a promising solution for transforming waste into new and highly sustainable construction materials according to alkali activation process. The unemployed fractions of boro-alumino-silicate pharmaceutical glass (BASG) and waste foundry sands (WFS) were employed in the production of synthetic conglomerates. Glass powders were firstly suspended into 'mild' NaOH/KOH aqueous solutions (2.5–5 M) for 180 minutes at 500 rpm, at room temperature or at 40°C. Conglomerates were later produced by embedding of foundry sands in slurries of alkali activated glass, for BASG:WFS ratios of 1:1, 1:2 or 1:3. The mass of sand embedded is a function of the grain size distribution. A final drying phase, lasting 7 days at 40°C, promoted the consolidation of the newly-formed materials due to the formation of strong siloxane bonds. The obtained conglomerates were mechanically tested under compression. Interestingly, the composites exhibited a compressive strength-to-density ratio comparable with commercial insulating lightweight concrete and Plaster of Paris. Moreover, the leachates from conglomerates were subjected to optical emission spectroscopy in inductively coupled plasma (ICP-OES) to verify the stabilization of hazardous elements. The methodology selected for the stabilization of pollutants is compliant with UNI EN 12457–2:2002. The results show that the release of critical pollutants (Ba, Cr, Cd, Co, Mo, Ni) was maintained below the European limits. The research highlights the possibility to manufacture conglomerates starting from waste raw materials. Furthermore, stabilizing activity towards hazardous elements is achieved by all composite materials.

1. Introduction

One of the primary challenges in the field of materials research is the development of innovative strategies for the recycling and waste valorization. New environmental regulations demand reduction of waste production and resource extraction, emphasizing the need of sustainable practice and process optimization. [1]

Significant amount of waste and greenhouse gas emission have been attributed to the production of building and construction materials, contributing for approximately 30 % to the overall emissions of CO_2 into the atmosphere. [2–4]

Besides concrete, steel is also a major contributor to pollution. [5] In facts, steel and iron making are energy and resources

* Corresponding author at: Department of Industrial Engineering, University of Padova, Padova, Italy
E-mail address: enrico.bernardo@unipd.it (E. Bernardo).

https://doi.org/10.1016/j.cscm.2024.e03538
Received 2 April 2024; Received in revised form 4 July 2024; Accepted 16 July 2024
Available online 23 July 2024

consuming processes, [6] a resulting in generation of massive amount of solid waste. [7–9] The substantial volume of waste foundry sands (WFS) has become a critical environmental issue. Due to the contamination with ferrous and non-ferrous metallic components as well as traces of pyrolyzed organic binder [10,11], any recycling process has been widely spread for exhausted sand. WFS are currently discarded in landfills [12] posing the risk of percolation of hazardous substance through the soil.

In order to work into an environmental conservation perspective, [13] several studies have explored the potential for replacing virgin raw materials with industrial by-products. Metallurgical scraps, such as waste slags [14] and/or foundry sands [15], are successfully incorporated in newly-formed products for the building sectors nowadays. Foundry sands are used in the construction sector as a viable fine aggregate alternative. Garcia et al. [16] have proposed a partial substitution of natural sand with WFS in concrete, yielding cost benefits around 10 %. Instead, Kumar et al. [17] developed a complete replacement of natural sand in concrete; due to limited workability, WFS-derived cement is not suitable for structural applications: several studies fixed at maximum 20–30 % the proper replacement of natural sands. [18] The 20 % of maximum substitution rate is further validated by the research of Prabhu et al. [5]

However, a new promising alternative is to use WFS for bricks manufacturing. Aneke *et. al* investigated the production of bricks by combining the use of WFS and plastic waste (PET) revealing a substantial improvement in mechanical performance [2] compared to clay bricks. Despite the limited scientific studies, there are pioneering bricks industries that utilize WFS. In fact, the green-bricks are suitable for use in single-story load-bearing building, as well as for infill walls in multi-story framed construction. [19]

Quite surprisingly, the glass industry shares the same recycling issues with the steel industry. Despite the general assumption that glass is fully recyclable, the global recycling rate of glass waste is below 30 %. Approximately 200 million tons of glass are annually landfilled, worsening the problem of natural resources supply [20,21]. The glass disposal is motivated by different aspects of glass life cycle. After use, glass articles are generally crushed in fragments and powders, later sorted by dimension and chemical composition. The finest fraction of glass cullet ('glass fines') is typically not accepted in 'close-loop' recycling, i.e. remelting for the manufacturing of new articles, according to the enhanced content of heterogeneities [22]. Moreover, glasses with different chemical composition should be prevented: they could lead to the formation of hazardous gas emission (e.g. PbO from cathode ray tube glasses, or fluorine from opal glasses) [23].

Currently, boro-alumino-silicate glass used in pharmaceutical packaging (in the manufacturing of vials and syringes) deserves specific attention. The production of articles based on this glass had an enormous increase, due to the high global demand stimulated by the Covid-19 emergency [24]. Glass vials after use (e.g. in hospitals) are not recovered at all; 'closed-loop' recycling is feasible with 'clean' material, deriving from defective containers ('production waste') after separation from metal and polymer pieces, realized by mechanical crushing and generation of unrecyclable, contaminated glass fines [25]. The contaminated fractions represent a waste management problem.

Again, the building industry is certainly attractive for 'open-loop recycling' (i.e. reuse in products not matching the original article) of inorganic residues, with limited energy inputs. Waste glass (WG) can be utilized as a replacement to traditional materials: [26] fine glass particles are suitable as aggregate in Portland cements. [27,28] Nevertheless, this alternative could be considered a 'downcycling' approach [29] due to lower reactivity and any valorization of final chemical composition.

To improve the suitability of the process and the quality of final construction materials ('up-cycling'), researchers have implemented reliable solutions. Aneke et al. [30–32] demonstrated the feasibility to produce eco-friendly bricks by mixing recycled crushed glass and scrap plastic. This methodology allows to avoid high temperature (1300 °C) necessary for the clay bricks production, since only 220 °C is required for plastic melting.

Even geopolymers and alkali activated materials represent a valid alternative for the up-cycling of WG. In fact, due to the concentration of SiO_2 and Al_2O_3, WG can be exploited to produce alkali-activated building materials [33,34]. Alkali activation focuses on the dissolution of silicate and alumino-silicate inorganic materials in highly concentrated aqueous solutions of alkali hydroxides and silicates; the resulting slurries undergo progressive hardening, at nearly room temperature according to condensation reactions between dissolution products and formation of a gel. Beyond glass, the process may involve different industrial byproducts (e.g. slags, ashes), replacing refined and natural derived raw materials, such as metakaolin [35]. A general goal in alkali activation is the development of highly durable gels, featuring a 'zeolite-like' network structure (from the bridging of SiO_4, AlO_4, BO_4 units), in products known as 'geopolymers', which may act as a 'cage' for heavy metal ions [36]. The reuse of inorganic waste is undoubtedly in favor of sustainability, but a weakness is represented by the significant amounts of alkali compounds, as activators.

Recent studies have already highlighted the potential of glass powders for alkali activation, supported by solutions of limited molarity (not exceeding 3 M NaOH or KOH) [37,38]. Such conditions ('mild' activation) do not correspond to extensive dissolution of the same glass, subjected only to surface alteration. Glass components are released in solution, but the gel determined by their polymerization is not significant for the binding of adjacent glass particles; these particles, on the contrary, are bridged by strong chemical bonds, arising from condensation of reactions involving hydrated surface layers (e.g. Si-O-Si bonds from the condensation of two SiOH groups, belonging to two distinct particles).

This work shows the feasibility of producing alkali-activated materials by the combination of pharmaceutical glass waste powder and discarded foundry sands. The novelty of this study is represented using pharmaceutical glass scarps as the only starting raw materials for 'mild' alkali activation of glass. WFS are embedded in large quantities into glass slurries, even up to 3 times [wt%] the starting glass powder.

The low molarity of the activating solution (2.5–5 M) together to hardening at very low temperature (T_{max}=40°C) are both aspects that converge to the higher sustainability of the final product. Despite the simple processing, hazardous elements are stabilized in dense products [39], totally avoiding a following thermal treatment. The obtained conglomerates could have application as building elements, replacing lightweight concrete blocks.

2. Materials and methods

This study is based on treatments performed on boro-alumino-silicate glass denoted as BASG (SiO_2= 76.1 wt%, B_2O_3=9.2 wt%, Al_2O_3=5.7 wt%, Na_2O=7.5 wt%, CaO=1.5 wt%, supplied by the company Stevanato Group (Piombino Dese, Padova, Italy). The chemical composition was obtained by XRF (Bruker S8 Tiger, X-ray fluorescence spectrometer, Bruker, Germany).

Three different types of waste foundry sands (referred to as S1, S2, S3), supplied by foundries located in Northern Italy (and collected by INSTM, Florence, Italy), were used as fillers. The elemental composition was assessed by SEM-EDS (SEM-EDS, FEI Quanta 200 ESEM, Eindhoven, Netherlands), as reported in Table 1.

BASG (supplied in coarse fragments) was first dry ball milled (Pulverisette 7 planetary ball mill, Fritsch, Idar-Oberstein, Germany) and then sieved, to collect fine powders (<75 μm), as typically used in alkali activated slurries [40]; sands were used in as received conditions. The particle size and the distribution particles (D_{50} and D_{90}) of foundry sands were determined by using Mastersizer 2000 Light Diffractometer (Malvern Panalytical, Malvern, UK).

Activation was achieved by suspending fine BASG powders in a sodium hydroxide/potassium hydroxide blended solution (2.5 M 50 mol% NaOH/50 mol% KOH in water) following previous experiences [37,38], or directly in sodium hydroxide solution (5 M NaOH in water). NaOH and KOH reagents had both been purchased from Honeywell (Charlotte, North Carolina, USA). BASG powders and activating solutions were used in a 60 %-40 % weight proportions; the suspensions were mechanically stirred for 180 minutes at 500 rpm, at room temperature or at 40°C, before drying.

Sand-containing composites were produced by repeating the same activation/mixing procedure adopted for pure BASG; just before drying glass suspensions were added with sands, according to the proportions shown in Table 2 (liquid kept in proportion with the glass content; the sand addition enhanced the solid content of the suspensions), and subjected to additional stirring (10 min at 500 rpm). The suspensions were finally dried, after pouring in polystyrene moulds, at 40°C for 7 days. The stability of all conglomerates was preliminarily assessed by immersion in distilled boiling water, for one hour.

Geometrical density (ρ_{geom}) was determined as the ratio between mass and volume measured by analytical balance and digital calliper. Helium pycnometer (Anton-Paar Ultrapyc 3000, Graz, Austria) was used to assess apparent density (ρ_{app}) and true density (ρ_{true}), in the form of solid and powdered samples respectively. Open, closed, and total porosity were inferred from the density data. The morphology of sands before and after inclusion in glass-based matrices was investigated by scanning electron microscopy (FEI Quanta 200 ESEM, Eindhoven, The Netherlands) equipped with EDS.

The evolution of samples was studied by means of Fourier-transformation infrared spectroscopy (FTIR) and X-ray diffraction analysis (XRD) on powdered samples. FTIR analysis were performed in the range 450–4000 cm^{-1} using 64 scans (Jasco 4200 FTIR spectrometer, Jasco, Japan). XRD analysis was conducted using Cu Kα radiation at 40 kV and 40 mA, and in the 2θ interval of 9–70°, with a step size of 0.02° and 2 s of counting time (D8 Advance, Bruker AXS, Karlsruhe, Germany). The patterns were subjected to semi-automatic phase detection, operated by the Match!® program package (Crystal Impact GbR, Bonn, Germany), supported by data from the PDF-2 database (ICDD-International Centre for Diffraction Data, Newtown Square, PA, USA).

The compressive strength of composites was determined by crushing studied cubic samples (15 mm × 15 mm × 15 mm), cut from bigger samples, using a universal testing machine (Quasar 25, Galdabini, S.p.A., Cardano al Campo, Italy), with a cross-speed of 1 mm/min. Strength and density data were compared to those of commercial materials by means of the Cambridge Engineering Selector (CES) software package (Granta EduPack, Ansys Granta, Canonsburg, PA, USA). Ashby's diagrams, introduced in the '80 s, are plots to determine the optimal relationship between the properties of the materials and/or processing routes. [41]

Composites were evaluated also in terms of stabilization of heavy metals. A leaching test was conducted on materials crushed below 4 mm and immersed in distilled water, to obtain a liquid-to-solid ratio of 10 (Norm EN 12457–2, 2002). The fragments, suspended in water, were kept under mechanical stirring, at room temperature, for 24 h. The liquid fraction, passing through a 0.4 μm filter, was later analysed by inductively coupled plasma – atomic emission spectrometry (ICP-AES, SPECTRO Analytical instrument GmbH, Kleve, Germany).

3. Results and discussion

3.1. Activation of glass powders

The alkaline activation of waste glass is object of debate [42]. A key role is undoubtedly played by OH^- ions, which determine the cleavage of Si-O-Si bonds, i.e. the main bonds in any silicate glass. The attack, in other words, has the potential to disrupt the whole glass structure, with all glass components released in solution. Obviously, the chemistry of released species depends on the glass composition. Condensation reactions may lead to newly formed phases, such as C-S-H for soda-lime [43]. Operating with solutions of

Table 1
– Chemical composition of sands, assessed by SEM-EDX.

Element [%]											
Sand	C	O	Na	Mg	Al	Si	S	K	Ca	Cr	Fe
S1	15.2	33.7	2.0	1.1	2.2	30.4	-	-	-	9.9	5.7
S2	52.4	28.8	0.5	0.7	3.9	11.2	0.4	0.3	0.8	-	1.0
S3	13.2	45.1	-	-	0.9	39.7	-	0.4	-	-	0.8

Table 2
– Summary of formulations and activation conditions.

Label	Sand	BASG-to-WFS [wt% / wt%]	Molarity [mol/l]	Temperature [°C]
C1.1	1	1:3	2.5	25
C1.2	1	1:3	2.5	40
C2.1	2	1:1	5	25
C2.2	2	1:1	5	40
C3.1	3	1:3	5	40
C3.2	3	1:2	5	40

limited molarity, we can think at a limited dissolution, with the hardening of activated glass suspensions not relying on the binding action of newly formed phases, but simply on condensation reactions of hydrated layers. Si-OH groups at the surface of one particle may react with Si-OH groups at the surface of another particle, forming Si-O-Si bridges. Components released in solution may as well undergo polymerization reactions, forming a gel, but the contribution to the consolidation is doubtful. Lago et al. [38] clearly showed the resistance of cold consolidated boro-alumino-silicate powders even to harsh conditions (pH=2), owing to the bonding of adjacent particles, while gel could be leached out.

Fig. 1, collecting the results of FT-IR spectroscopy analysis, provides a further confirmation of the behavior of boro-alumino-silicate glass, subjected to alkali activation, with the support of previous literature [44,45]. The starting material exhibits typical bands related to Si-O-Si and Si-O-Al asymmetric stretching vibrations (centered approximately at 1000 cm^{-1}), $[BO_4]^-$ vibration and Si-O-B stretching vibration (hump-like signal at 925 cm^{-1}), Si-O-Si symmetric stretching vibration and $[BO_3]$ vibration (peaks at 705–670 cm^{-1}) and Si-O-Si bending (450 cm^{-1}). Moreover, the band at 790 cm^{-1} is assigned to the symmetric stretching vibration of O-Si-O [46]. The alkali activation of the material may be inferred from the downshift of the main peak due to mixed-ion gel formation (980 cm^{-1}) [47], along with a new signal related to the formation of carbonates (1450 cm^{-1}).

After immersion in boiling water, activated BASG samples did not disintegrate. Interestingly, the FT-IR spectrum of the material after boiling is practically identical to that of the starting material. We can assume that the modification of the FT-IR spectrum, with activation, derived from the overlapping of signals from nearly unmodified glass and extra phases, such as alkali carbonates and gel, from the collection of components released in solution according to partial disruption of glass network (silicate, borate, and aluminate ions). The high alkali content of this gel likely determined a low network connectivity (i.e. a limited number of bridging oxygens), and consequently a poor chemical stability.

The stability of 'skeletons' of mutually welded glass particles was further assessed by applying boiling tests on samples activated in more aggressive conditions, i.e. increased temperature (from 25 to 40 °C) and molarity (passing from 3 M of mixed NaOH-KOH solution to 5 M of NaOH solution) [48], both pH and temperature have significant influence on the mechanism of alkali activation reaction. Again, the FT-IR spectra for 'boiled' samples (not shown) were nearly undistinguishable from that of unreacted glass. The harsher dissolution conditions had some visible effects only on activated materials, as testified by Fig. 1b. More precisely, the carbonate-related band (1450 cm^{-1}) increased with increasing processing temperature, whereas higher molarity promoted a slight enhancement of the band at 859 cm^{-1}, assigned to stretching vibrations of B–O bonds in BO_4 tetrahedral unit [49]. The more intense attack (involving more OH^- ions) likely determined an increased release of borates, forming more BO_4 units in the gel. Despite this, the

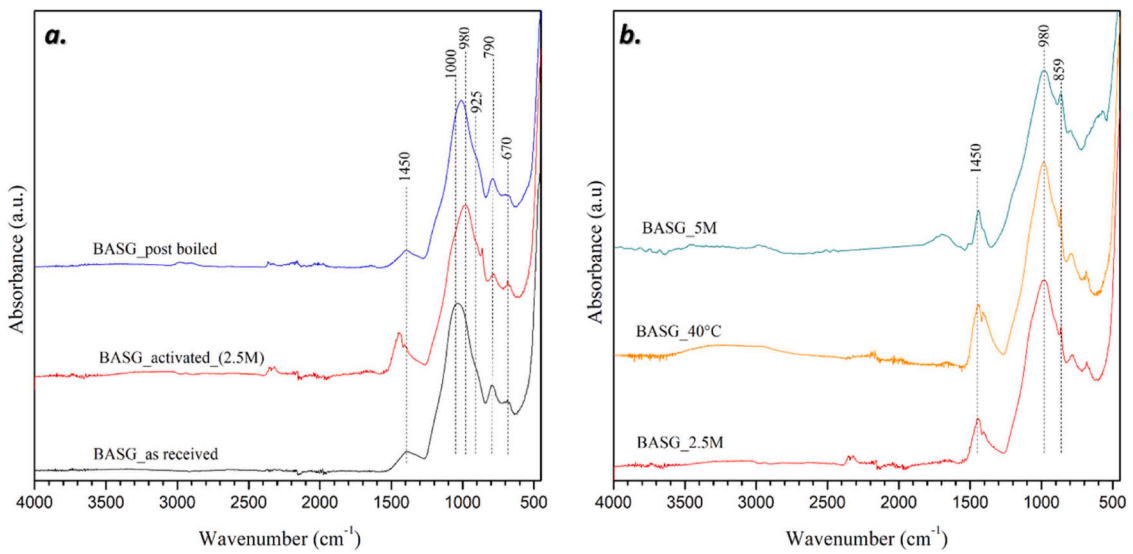

Fig. 1. . - FTIR of boro-alumino-silicate glass (a) in as received condition, activated and after boiling test (b) alkali activated 2.5 (T_{room}), 2.5 M (40°C) and 5 M (T_{room}).

gel remained soluble.

Harsher activation conditions reasonably enhanced the surface hydration. With increased Si-OH groups, the welding of adjacent particles, by condensation, was favored. As illustrated by Fig. 2 and Fig. 3b, the compressive strength of alkali activated BASG nearly doubled (from approximately 20 MPa to 40 MPa) by increasing molarity or the process temperature. In addition, it must be noted that the developed materials, in all conditions, were much stronger than conventional commercial construction materials in the same density range, such as plaster of Paris and lightweight concrete. Porosity and compressive strength data of BASG alkali activated were reported in Fig. 3.

The conglomerates exhibited inferior mechanical properties relative to those of glass matrices, as shown in Fig. 2 and Fig. 3(a). However, a comparative analysis had revealed that the newly created materials were in the range of existing insulating lightweight concrete.

Moreover, mechanical properties of obtained composite alkali activated materials have been compared with the previous research in this field (Table 3). To establish the most representative benchmarks, studies with an integration of sands that exceed 50 % by weight is sought.

A crucial aspect is represented by the binder, specifically the material that will be employed to encapsulate and consolidate the WFS. The lack of embedding material [50] is not a viable solution, as it will compromise the mechanical functionality of the product; contrarily, the use of foundry sands as fine aggregate substitutes in the cement [51], has been demonstrated to be a feasible option, with a reported 18 % decrease in compressive strength when 60 % of WFS is incorporated into the mixture. The same conclusions are also drawn by Khatib et al. [52]. The addition of WFS in concrete results in a reduction in workability and strength.

Aneke et al. [4,15,31] have instead developed a technique that enable the production of composite green-brick, incorporating WFS into waste polyethylene terephthalate (PET) plastic. The compressive strength is approximately 40 MPa, demonstrating a higher value than traditional clay bricks. The process temperature, however, is the critical point, as it is necessary to reach 220°C to melt the plastic.

Of course, geopolymers, exhibits a high degree of similarity to the materials produced in the current study. Sgarlata et al. [53] investigated the use of metakaolin as a binder, achieving mechanical characteristics comparable to those listed in this paper (Table 3). Considering the perspective of waste management, metakaolin is an energy consuming material, since it is produced by the calcination of kaolin at high temperatures [T=600–850°C]; moreover, the molarity of the alkaline solution fixed at 8 mol/L, places additional constraints on the ecological and safety performance of the final AAMs product. Starting from a different binder the same issue of high temperature treatment is shared by Ferrazzo et al. [54], while Apithanyasai et al. [55], although the unequivocally superior mechanical properties, work with high molarity of alkaline solution [NaOH, 8 M].

3.1.1. Inclusion of sands

The studied sands were different from each other not just in terms of chemical composition but also in terms of morphology, as illustrated by Fig. 4.

The surface area of the solid raw material is a key aspect in the formulation of batches for alkali activation and in general, for any cementitious blend [56], so a precise determination of particle size distribution was needed, beyond SEM observation. The distribution curves and the cumulative curves are shown in Fig. 5a and Fig. 5b, respectively.

It is evident that S1 consisted of quite coarse particles, with a nearly mono-modal size distribution (centered at 400 μm); the

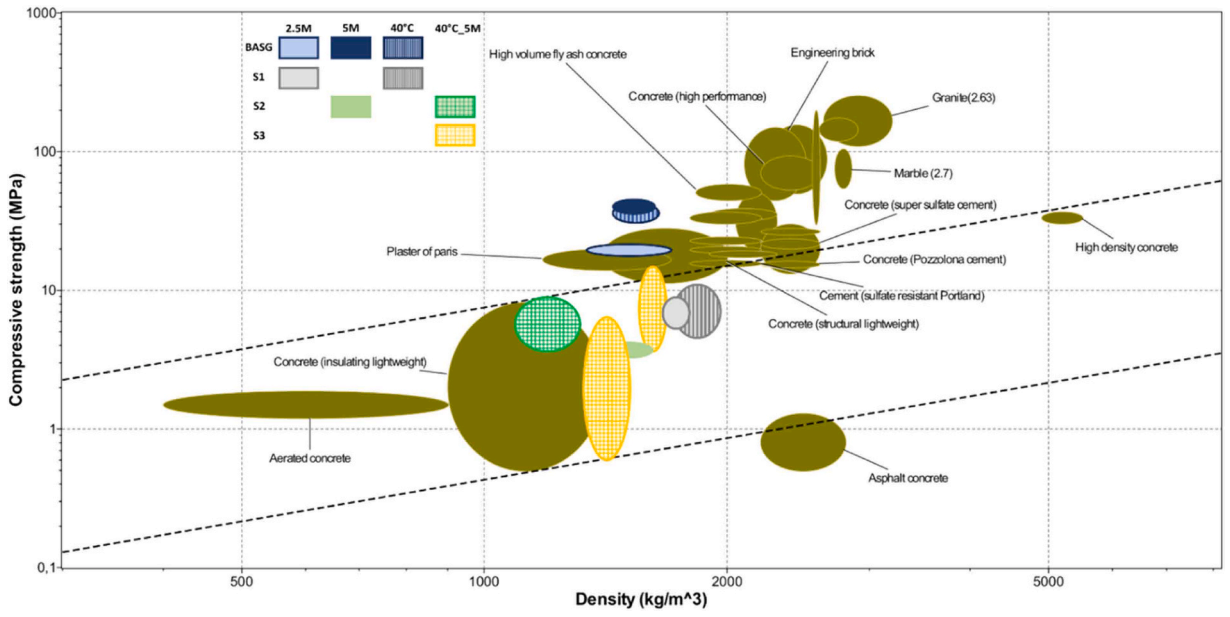

Fig. 2. Compressive strength/density trade-off of glass matrices and new conglomerates (computed by means of CES software package).

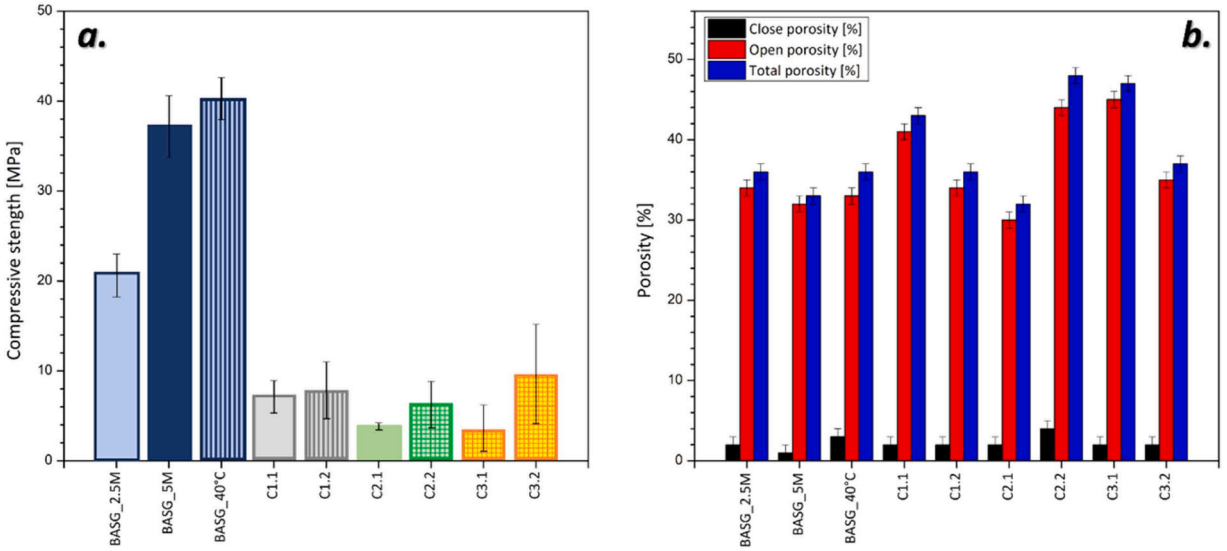

Fig. 3. (a) Compressive strength and (b) porosity (open, close and total) of BASG alkali activated and all conglomerates.

Table 3
Mechanical properties of obtained materials compared with similar research on same field.

WFS [%]	Binder	t_{curing} [days]	T_{curing} [°C]	σ_c [MPa]	ρ_{geom} [g/cm^3]	Reference
70	NaOH	28	75	1.0	1.50	[50]
60	Concrete	28	RT	29.9	-	[51]
60	Concrete	28	RT	32.9	-	[52]
70	Metakaolin geopolymer	28	RT	8.5	-	[53]
68	sugar cane bagasse ash-eggshell lime alkali-activated	28	40	9.8	-	[54]
70	Fly ash alkali-activated	28	RT	18.9	-	[55]
70	Plastic scraps [PET]	-	220	38.14	2.24	[2]
70	Plastic scraps [PET]	-	220	36.18	1.83	[15,31]

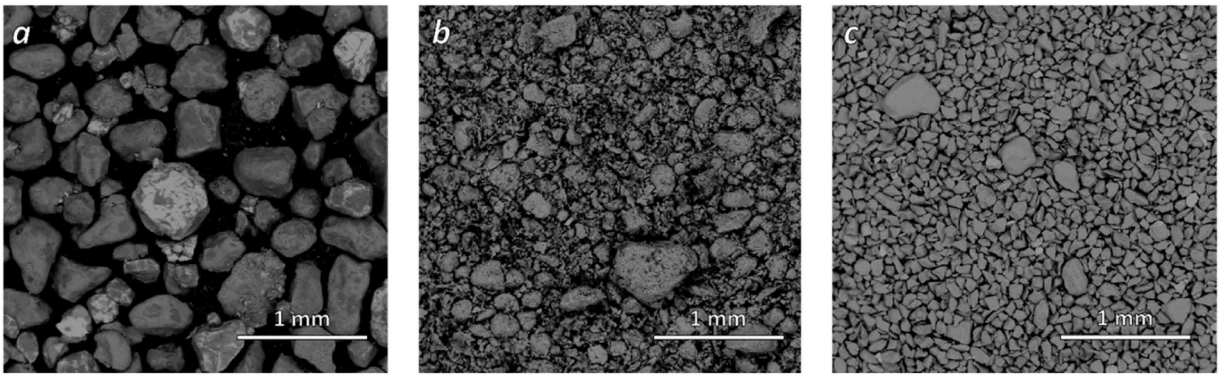

Fig. 4. SEM micrographs of a) S1, b) S2 and c) S3, in as received conditions.

minimized surface area minimized the interaction with the matrix, allowing for the inclusion of great quantities of sand [33],as reported by Table 2. Mixtures remained quite fluid even for a sand/glass ratio of 3. Since the amount of attacking solution was calibrated to the amount of glass, formulations at high sand content determined a substantial 'dilution' of activators (NaOH and KOH). S3 was undoubtedly finer, but still offered a mono-modal size distribution (centered at 120 μm). With the finest particles remaining above 40 μm, S3 could be mixed with BASG powders again up to a sand/glass ratio equal to 3. On the contrary, S2 featured a bi-modal size distribution [57], including a fraction of powders well below 40 μm: the enhanced interaction with the matrix, from enhanced surface area, impeded the inclusion of sand in big amounts; the sand/glass ratio did not exceed 1. The characteristic particle diameters D50 and D90 and the true density of sand are summarized in Table 4.

Granulometric analysis was necessary to elucidate the incorporation mechanism of filler particles (WFS) into alkali activated

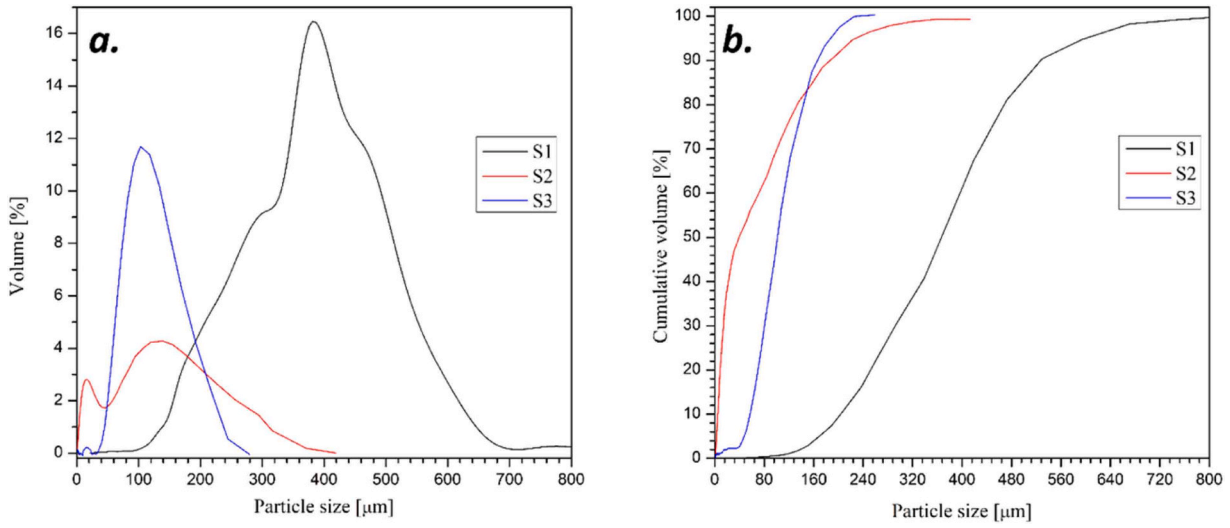

Fig. 5. - Particle size distribution of sands.

matrices. Contrary to other studies [55], these authors incorporated the foundry sands in 'as-received' condition, avoiding any sieving or grading procedure. The choice is consistent with the economic assessment made by Fiore et al. [58]. In fact, sieving operation and potential milling request energy consumption and extra cost, which contravenes the environment sustainability aim.

Some differences between sands were detected also in term of mineralogy. As shown by Fig. 6, α-quartz [SiO_2, PDF#461045] was the main crystal phase in all case. However, secondary minerals could be recognized. S1 showed diffraction maxima attributable to iron oxide [Magnetite, Fe_3O_4, PDF#750449 or related solid solutions], reasonably from oxidation of casted metal. Such contamination is consistent with the lightly coloured particles in Fig. 5. In S2, mineral contaminations were imputable to sodium magnesium aluminum silicate hydroxide hydrate [montmorillonite, $(Na,Ca)_{0.33}(Al,Mg)_2Si_4O_{10}(OH)_2{\cdot}n$H2O, PDF#020014], that is the main component of bentonite; bentonite is the largely used moulding-sand binder in the foundry industry [59], because of good demoulding capacity, excellent air permeability and stability in high-temperature environments [60]. Finally, S3 had diffraction maxima ascribable to potassium alumino-silicate [microcline, $KAlSi_3O_8$, PDF#220687], a mineral belonging to the feldspar group typically accompanying quartz in iron casting moulds [61].

3.1.2. Composites embedding S1

Despite the 'dilution' of glass and related activators, the samples from inclusion of S1 (C1.1 and C1.2) survived to boiling test and exhibited a strength-density ratio falling between the limits for insulating lightweight concrete. More precisely, in Fig. 2 the dashed lines correspond, respectively, to the minimum and maximum values of the strength-density ratio of commercial insulating lightweight concrete, according to data stored in the database of CES software package. Contrary to concrete, the inclusion of fillers did not enhance the compressive strength; this can be understood as an effect of the above-mentioned dilution and by the establishment of weaker bonds between glass and sand powders, compared to those between just glass powders. This fact is in turn reasonable: crystalline silica (in quartz) is far less reactive than amorphous silica [62].

The absence of substantial dissolution of quartz is testified by Fig. 7. The intensity of diffraction lines is reduced, passing from sand to activated composite, in agreement with the dilution of sand with BASG (25 wt% of the solid). No change could be observed after boiling.

In terms of morphology, BASG glass did not form a uniform layer on sand particles, as shown by Fig. 8, confirming the establishment of a quite weak interface. In any case, quartz and glass formed a matrix embedding metal particles (composition shown in Fig. 8a). Iron- and chromium-containing particles were easily recognized by SEM-EDX. We cannot exclude the presence of both oxide particles (featuring both Fe and Cr, likely Cr-magnetite solid solution, Fig. 8b) and metallic particles (Fe-based, Fig. 8c). The inclusions did not lead to gradients in the colouration, which remained light gray (Fig. 9).

Table 4 -
Dimension of particles and true density of foundry sands.

Sand	D50 [μm]	D90 [μm]	True density [g/cm^3]
S1	366.66	527.16	3.13
S2	39.32	186.62	2.08
S3	101.25	166.23	2.70

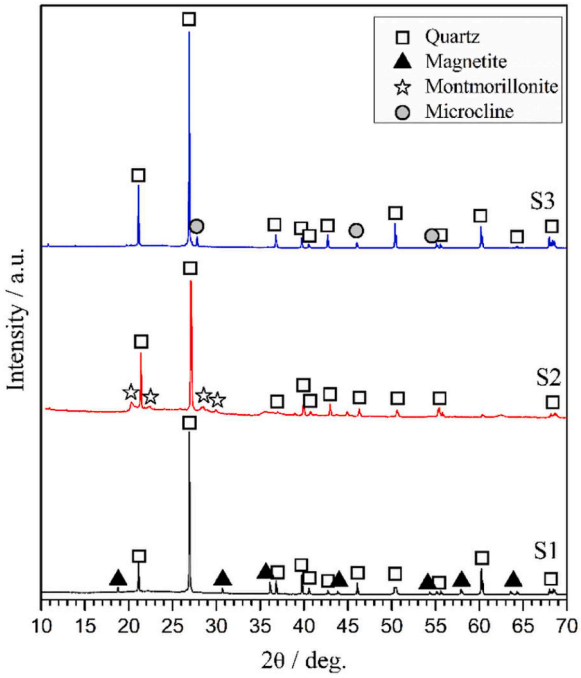

Fig. 6. X-ray diffraction analysis of waste foundry sand, in the as received conditions.

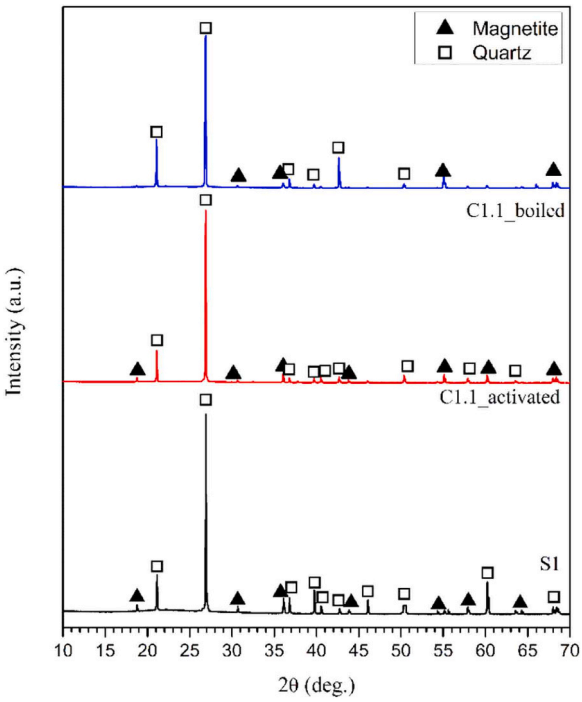

Fig. 7. XRD diffraction patterns of S1 compared with its corresponding conglomerate C1.1 before and after boiling test.

3.1.3. S2 and S3-based composites

In the handling of S2, the presence of a very fine fraction complicated the activation. It has been already observed that with high surface area, the enhanced interaction determines some form of alkaline absorption, reducing the embedding effectiveness [63]. In order to overcome these limits, considering the expected limited presence of toxic impurities, composites involving S2 underwent activation in harsher conditions (higher molarity of the solution and/or higher reaction temperature), previously avoided for S1, in

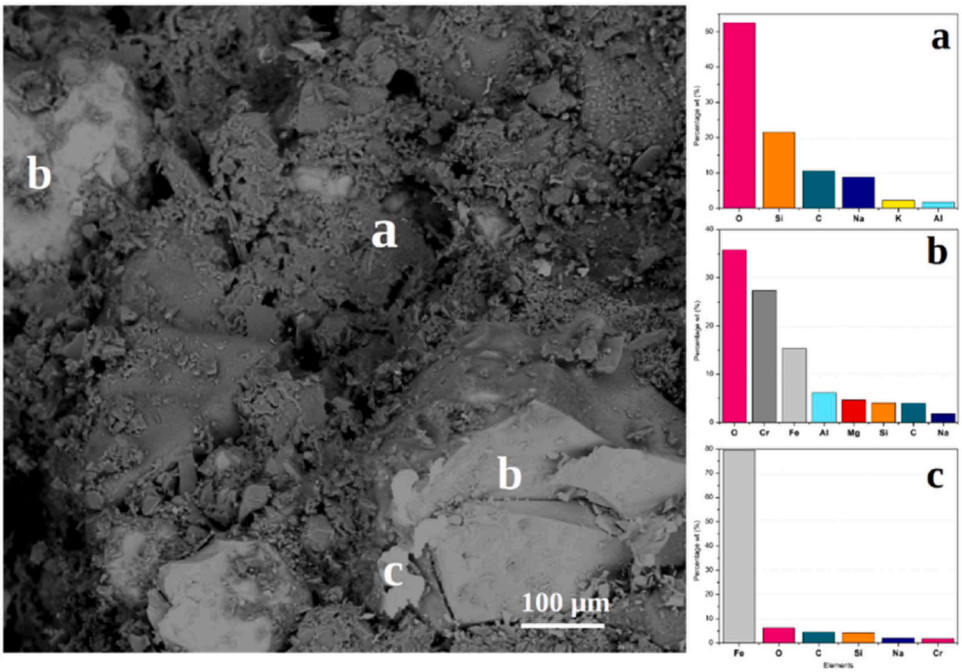

Fig. 8. SEM-EDX analysis of the C1.1 composite; a matrix comprising quartz inclusions (a) embeds metal particles (b: iron rich, c: chromium rich).

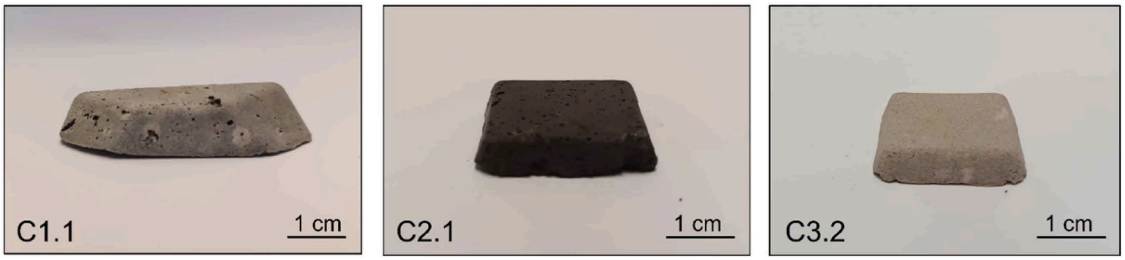

Fig. 9. Visual aspect of foundry sand-embedding composites (from left to right: C1.1, C2.1 and C3.2).

order to limit the dispersion of heavy metals. S3, also featuring quite fine powders, was handled similarly to S2.

In general, harsher condition led to a more compact matrix. S2 featured a quite extensive carbon contaminations (due to incomplete pyrolysis of resins during the sand-casting process), resulting in coarse clusters (Fig. 10a) as well as in smaller particles trapped in the matrix (Fig. 9b). Carbon inclusion motivate the dark colouration, visible from Fig. 9.

Composites embedding S3 still featured carbon contaminations (Fig. 11a), but in form of small, isolated zones. The overall colouration was gray-pink (Fig. 9). Such tones could be justified by the iron content (Fig. 11b).

Contrary to composites embedding S1, composites featuring S2 and S3 had some chemical interactions. As shown by Fig. 12, the main diffraction line corresponding to quartz had an anomalous increase with activation. This can be justified only as the result of the overlapping, in the same position, of signal from an additional, newly formed phase. A reasonable contribution is that provided by gismondine [$CaAl_2Si_2O_8{\cdot}4\ H_2O$, PDF#200452]. This phase disappeared with boiling, consistent with the literature on its limited durability [36,64].

Also composites from S2 and S3 could be attractive as new, sustainable construction materials (see Fig. 2, Fig. 3a). The samples fall again between the minimum and maximum values of the strength-density ratio of porous, insulating concrete. Some S2-based samples (C2.2) even exhibit some overlapping of strength and density values, to those of the specific type of concrete.

3.2. Stabilisation of pollutants

Alkali-activated materials are becoming more and more important in the perspective of stabilization of pollutant. [65] The alkali activated glass is renowned for its potent ability to immobilized hazardous elements as demonstrated by Lago et al. [39] and Monich et al. [66]; however, both the studies assume the application of thermal processing, including sintering treatment. In the present paper, the stabilization of hazardous elements is achieved even at room temperature. In fact, all composites were verified according to the

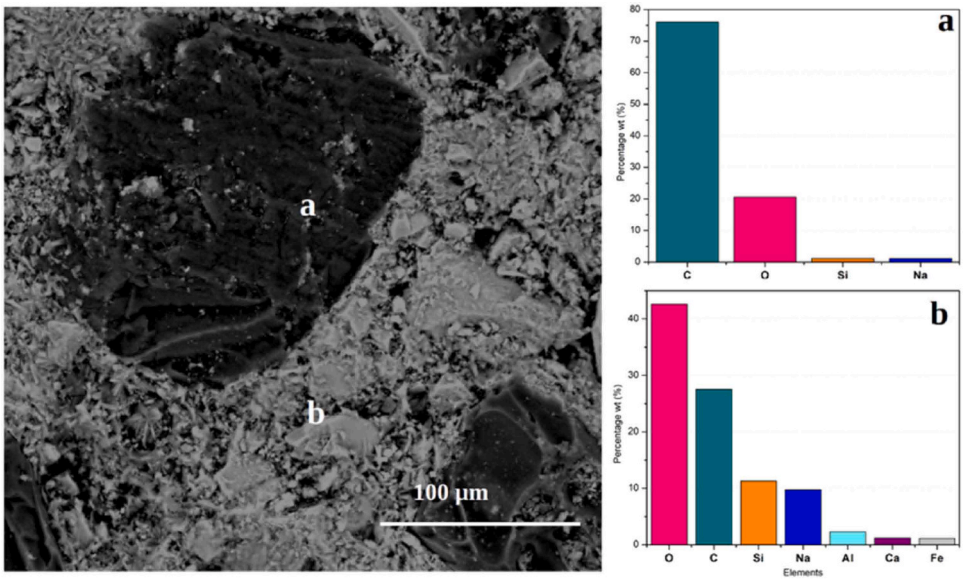

Fig. 10. SEM micrograph and SEM-EDX analyses of C2.2 composite (S2, embedded in BASG activated at 40 °C, by 5 M NaOH solution): a) C-rich inclusion; b) matrix.

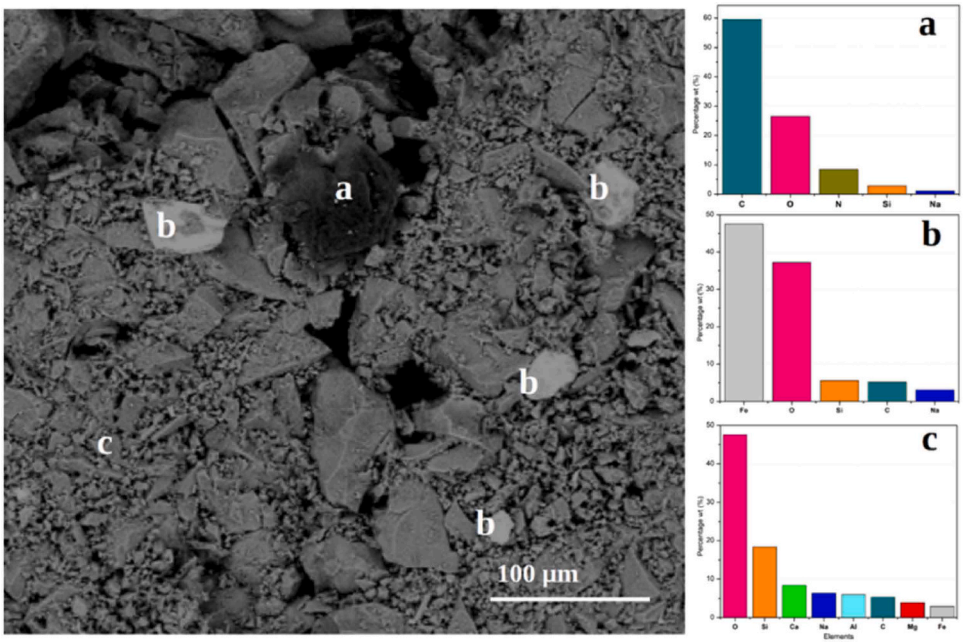

Fig. 11. SEM micrograph and SEM-EDX analyses of C3.2 composite (S3, embedded in BASG activated at 40 °C, by 5 M NaOH solution): a) C-rich inclusion; b) Fe-rich inclusion; c) matrix.

application of European standard UNI EN 12457–2:2002 [67]. This standard is used in Italy to assess the disposal or reuse of the waste [68].

Despite not resulting from extensive dissolution of constituents, the developed composite materials exhibited a nearly negligible release of heavy metals. Iron and chromium, effectively detected in several inclusions, made no exception. The release was more than one order of magnitude below the limit for inert materials, as shown by the overview of Fig. 13, except for vanadium, released at maximum rate corresponding to 50 % of the limit for inert materials.

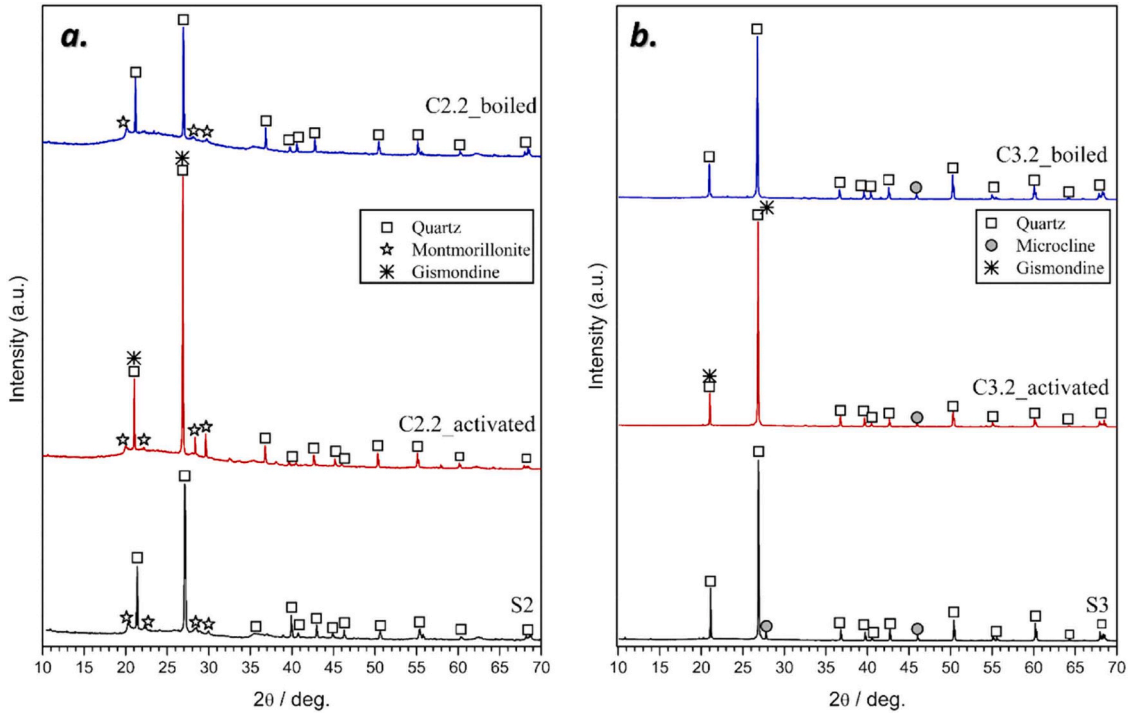

Fig. 12. XRD diffraction patterns of composites embedding S2 (C2.2) and S3 (C3.2).

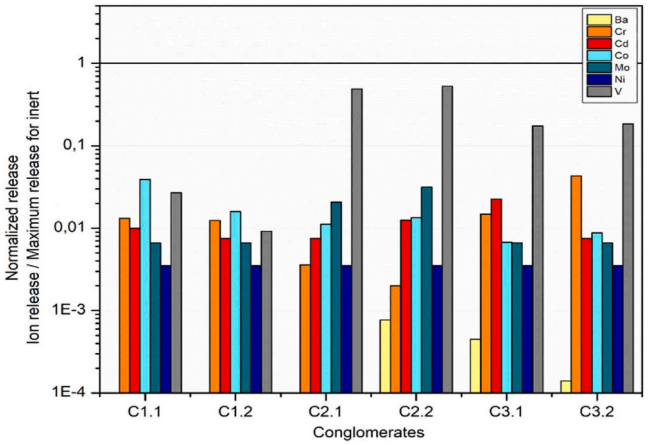

Fig. 13. - Logarithmic graph regarding the concentration of heavy metals on the leachate solutions, detected by ICP, normalized on the related limits for inert materials according to UNI EN 12457–2:2002 (the value 1 corresponds to a metal released at the maximum level for classification as inert).

4. Conclusions

The alkali activation of pharmaceutical glass emerges as a tool for both stabilization of waste foundry sands and development of highly sustainable construction materials. The sustainability derives from the combination of two forms of inorganic waste, with minimization of inputs in terms of materials (e.g. alkali activators, dramatically reduced in composites featuring a high sand/glass ratio) and energy. Alkali activated glass shows great versatility in embedding fillers. The obtainment of building materials has been successfully accomplished with sands that considerably differs themselves in granulometry and chemical compositions. Correlations have also been highlighted between experimental variables and final products: the concentration of the activating solution [2.5–5 M] and the mixing temperature [T= 25–40°C] is directly proportional both to filler embedding ability, and to the final mechanical properties of the obtained materials. The alkali-activated glass exhibits compressive strength exceeding 40 MPa; the embedding of foundry sands, enables the production of conglomerates (C1.2 and C3.2) with compressive strength approaching 10 MPa.

Moreover, BASG binder demonstrated an unprecedented stabilizing activity towards inorganic toxic pollutants, even at room temperate. Despite the high mass fraction of toxic elements such as Cr (see Table 1) and the variable activation conditions (concentration of alkali hydroxides, temperature, amount of sand introduced in glass suspensions), leaching test shown values significant below the range fixed for inert materials. These remarkable results fit the targets highlighted by new European guidelines on hazardous industrial waste in the Union [69].

Further investigations will be focused on different technological aspects. First, a wider range of durability experiments should be explored to better compare the material with the current commercial solutions: over the boiling and compressive strength tests, analyses such as freeze-thaw cycles, resistance to chemical attacks, thermal shock and abrasive wear tests would be useful sources of information for this purpose. Also, the impact of the interplay between contaminants in inorganic waste and in glass will be the object of future investigations, adopting different waste materials as fillers. The flexibility and the simplicity of the approach is undoubtedly interesting in the perspective of incorporation of other inorganic waste as well as of recovery of pharmaceutical glass dismantled in big quantities but still not reused (e.g. glass from containers used in hospitals).

The main conclusions of the research can be summarized as follows:

- An effective low-cost and energy-saving strategy for 'up-cycling' boro-alumino-silicate glass and foundry sands wastes has been successfully developed.
- The glass-based binder obtained through alkali-activation proved efficient stabilizing activity towards hazardous heavy metal contaminants, according to current UNI EN 12457–2:2002 standard.
- Concentration and temperature of the activating solution, together with granulometry of inert material, have been recognized as determining factors regarding the stabilization offered by the waste-derived binder.

CRediT authorship contribution statement

Francesco Cammelli: Writing – original draft, Visualization, Validation, Methodology, Investigation, Data curation. **Enrico Bernardo:** Writing – review & editing, Supervision, Methodology, Funding acquisition, Conceptualization. **Giulia Tameni:** Writing – original draft, Visualization, Validation, Methodology, Investigation, Data curation.

Declaration of Competing Interest

The authors declare the following financial interests/personal relationships which may be considered as potential competing interests: Francesco Cammelli reports financial support was provided by INSTM (Consorzio Interuniversitario Nazionale per la Scienza e Tecnologia dei Materiali). If there are other authors, they declare that they have no known competing financial interests or personal relationships that could have appeared to influence the work reported in this paper

Data availability

Data will be made available on request.

Acknowledgments

Authors kindly acknowledge Ph.D. Annalisa Zacco for contributing on the granulometric analyses, M.Sc. Federico Zorzi for SEM analyses and M.Sc. Giulia Zanmarchi for ICP-OES analysis. This work was supported by: National project MUR PON R&I [2014–2021]; "SusPIRe" (Sustainable porous ceramics from inorganic residues) project [University of Padova, Department of Industrial Engineering, BIRD202134, 2021]; INSTM (Consorzio Interuniversitario Nazionale per la Scienza e Tecnologia dei Materiali) through CaRiPLo project 'New recycling process for the foundry sands: innovation aimed to get materials with high added value' [2020–1216].

References

[1] N. Pajunen, L. Rintala, J. Aromaa, K. Heiskanen, Recycling – the importance of understanding the complexity of the issue, Int. J. Sustain. Eng. 9 (2) (2016) 93–106, https://doi.org/10.1080/19397038.2015.1069416.
[2] F.I. Aneke, C. Shabangu, Green-efficient masonry bricks produced from scrap plastic waste and foundry sand, Case Stud. Constr. Mater. (2021) e00515, https://doi.org/10.1016/j.cscm.2021.e00515.
[3] Y.H. Labaran, V.S. Mathur, S.U. Muhammad, A.A. Musa, Carbon footprint management: a review of construction industry, Clean. Eng. Technol. 9 (2022) 100531, https://doi.org/10.1016/j.clet.2022.100531.
[4] M. Dabaieh, J. Heinonen, D. El-Mahdy, D.M. Hassan, A comparative study of life cycle carbon emissions and embodied energy between sun-dried bricks and fired clay bricks, J. Clean. Prod. (2020) 122998, https://doi.org/10.1016/j.jclepro.2020.122998.
[5] H.A. Subhani, R.A. Khushnood, S. Shakeel, Synthesis of recycled bricks containing mixed plastic waste and foundry sand: physico-mechanical investigation, Constr. Build. Mater. 416 (2021) 135197, https://doi.org/10.1016/j.conbuildmat.2024.135197.
[6] A. Bhardwaj, P. Kumar, S. Siddique, A. Shukla, Comprehensive review on utilization of waste foundry sand in concrete, Eur. J. Environ. 27 (3) (2023) 1056–1087, https://doi.org/10.1080/19648189.2022.2070778.
[7] P.P.O.L. Dyer, M. Geimba de Lima, Const. Build. Mat, Waste Foundry sand hot Mix Asph.: A Rev. 359 (2022) 129342, https://doi.org/10.1016/j.conbuildmat.2022.129342.
[8] J. Ahmad, Z. Zhou, R. Martínez-García, N.I. Vatin, J. De-Prado-Gil, M.A. El-Shorbagy, Waste foundry sand in concrete, production instead of natural river sand: a review, Materials 15 (2022) 2365, https://doi.org/10.3390/ma15072365.

[9] Global Foundry Report , (2019), Global Foundry Report. World Foundry Organization, England, UK. ⟨https://www.thewfo.com/news/global-foundry-report-2019/⟩ (accessed 18.03.2024).
[10] F. Cioli, A. Abbà, C. Alias, S. Sorlini, Reuse or disposal of waste foundry sand: an insight into environmental aspects, Appl. Sci. 12 (13) (2022) 6420, https://doi.org/10.3390/app12136420.
[11] J. Mitterpach, E. Hroncova, J. Ladomerský, K. Balco, Environmental analysis of waste foundry sand via life cycle assessment, Environ. Sci. Pollut. Res. 24 (2017) 3153–3162, https://doi.org/10.1007/s11356-016-8085-z.
[12] M.R. Sabour, G. Derhamjani, M. Akbari, A.M. Hatami, Global trends and status in waste foundry sand management research during the years 1971-2020: a systematic analysis, Environ. Sci. Pollut. Res. 28 (2021) 37312–37321, https://doi.org/10.1007/s11356-021-13251-8.
[13] L. Valentini, Sustainable sourcing of raw materials for the built environment, Mater. Today (2023), https://doi.org/10.1016/j.matpr.2023.07.308.
[14] S. Meshram, S.P. Raut, K. Ansari, M. Madurwar, M. Daniyal, M.A. Khan, V. Katare, A.H. Khan, N.A. Khan, M.A. Hasan, Waste slags as sustainable construction materials: a compressive review on physico mechanical properties, J. Mater. Res. Technol. 23 (2023) 5821–5845, https://doi.org/10.1016/j.jmrt.2023.02.176.
[15] F.I. Aneke, B.O. Awuzie, M.M. Mostafa, C. Okorafor, *Mater.*, Durability assessment and microstructure of high-strength performance bricks produced from pet waste and foundry sand, Materials 14 (19) (2021) 5635, https://doi.org/10.3390/ma14195635.
[16] G. García, R. Cabrera, J. Rolón, R. Pichardo, C. Thomas, Systematic review on the use of waste foundry sand as a partial replacement of natural sand in concrete, Const. Build. Mater. 430 (2024) 136460, https://doi.org/10.1016/j.conbuildmat.2024.136460.
[17] S. Kumar, R. Silori, S. Kumar Sethy, Insight into the perspectives of waste foundry sand as a partial or full replacement of fine aggregate in concrete, Sci. Total Environ. 6 (2023) 100048, https://doi.org/10.1016/j.totert.2023.100048.
[18] G. Prabhu G, J.H. Hyun, Y.-Y. Kim, Effects of foundry sand as a fine aggregate in concrete production, Const. Build. Mater. 60 (2014) 514–521, https://doi.org/10.1016/j.conbuildmat.2014.07.070.
[19] N. Hossiney, P. Das, M.K. Mohan, J. George, In-plant production of bricks containing waste foundry sand—A study with Belgaum foundry industry, e00170, Case Stud. Constr. Mater. 2018 (9) (2018), https://doi.org/10.1016/j.cscm.2018.e00170.
[20] Y. Huang, Z. Chen, Y. Liu, J.X. Lu, Z. Bian, M. Yio, C. Cheeseman, F. Wang, C.S. Poon, Recycling of waste glass and incinerated sewage sludge ash in glass-ceramics, Waste Manag. 174 (2024) 229–239, https://doi.org/10.1016/j.wasman.2023.12.007.
[21] J.L. Santana-Carillo, O. Burciaga-Díaz, J.I. Escalante-Garcia, Blended limestone-Portland cement binders enhanced by waste glass based and commercial sodium silicate - Effect on properties and CO2 emissions, Cem. Concr. Compos. 126 (2022) 104363, https://doi.org/10.1016/j.cemconcomp.2021.104364.
[22] M. Flood, L. Fennessy, S. Lockrey, A. Avendano, J. Glover, E. Kandare, T. Bhat, Glass fines: a review of cleaning and up-cycling possibilities, J. Clean. Prod. 267 (2020) 121875, https://doi.org/10.1016/j.jclepro.2020.121875.
[23] W.-J. Long, X. Zhang, J. Xie, S. Kou, Q. Luo, J. Wei, C. Lin, G.-L. Feng, Recycling of waste cathode ray tube glass through fly ash-slag geopolymer mortar, Const. Build. Mater. 322 (2022) 126454, https://doi.org/10.1016/j.conbuildmat.2022.126454.
[24] F. Bassani, C. Rodrigues, F. Freire, Life cycle assessment of pharmaceutical packaging addressing end-of-life alternatives, Waste Manag. 175 (2024) 1–11, https://doi.org/10.1016/j.wasman.2023.12.022.
[25] J.J. Klemeš, P. Jiang, Y.V. Fan, A. Bokjari, X.-C. Wang, COVID-19 pandemics Stage II – Energy and environmental impacts of vaccination, Renew. Sust. Energ. Rev. 150 (2021) 111400, https://doi.org/10.1016/j.rser.2021.111400.
[26] D. Robert, E. Baez, S. Setunge, A new technology of transforming recycled glass waste to construction components, Constr. Build. Mater. 313 (2021) 125539, https://doi.org/10.1016/j.conbuildmat.2021.125539.
[27] M. Carsana, M. Frassoni, L. Bertolini, Comparison of ground waste glass with other supplementary cementitious material, Cem. Concr. Compos. 45 (2014) 39–45, https://doi.org/10.1016/j.cemconcomp.2013.09.005.
[28] X. Jiang, R. Xiao, Y. Bai, B. Huang, Y. Ma, Influence of waste glass powder as a supplementary cementitious material (SCM) on physical and mechanical properties of cement paste under high temperatures, J. Clean. Prod. 340 (2022) 130778, https://doi.org/10.1016/j.jclepro.2022.130778.
[29] J.M. Allwood, Squaring the circular economy, Handb. Recycl. (2014) 445–477, https://doi.org/10.1016/b978-0-12-396459-5.00030-1.
[30] F.I. Aneke, B.O. Awuzie, Conversion of industrial wastes into marginal construction materials, Acta Structilia 14 (19) (2018) 119–137, https://doi.org.10.18820/24150487/as25i2.5.
[31] F.I. Aneke, N. Abdolhossein, Utilization of plastic waste material in masonry bricks production towards strength, durability and environmental sustainability, J. Sustain. Archit. Civ. Eng. 30 (1) (2022) 121–141, https://doi.org/10.5755/j01.sace.30.1.29495.
[32] A.F. Ikechukwu, C. Shabangu, Strength and durability performance of masonry bricks produced with crushed glass and melted PET plastics, Case Stud. Constr. Mater. 14 (2021) e00542, https://doi.org/10.1016/j.cscm.2021.e00542.
[33] Y. Lv, Y. Wang, D. Zuo, Effects of particle size on dynamic constitutive relation and energy absorption of calcareous sand, Powder Technol. 356 (2019) 21–30, https://doi.org/10.1016/j.powtec.2019.07.088.
[34] R. Xiao, Y. Ma, M. Zhang, Y. Zhang, Y. Wang, B. Huang, Q. He, Strength, microstructure, efflorescence behavior and environmental impacts of waste glass geopolymers cured at ambient temperature, J. Clean. Prod. 252 (2020) 119610, https://doi.org/10.1016/j.jclepro.2019.119610.
[35] T. Luukkonen, Alkali-activated materials in environmental technology: introduction. Alkali-Activated Materials in Environmental Technology Applications, Woodhead Publishing, Cambridge, 2022, pp. 1–12, https://doi.org/10.1016/B978-0-323-88438-9.00011-9.
[36] I. Lancellotti, M. Cannio, F. Bollino, M. Catauro, L. Barbieri, C. Leonelli, Geopolymers: An option for the valorization of incinerator bottom ash derived “end of waste”, Ceram. Int. 41 (2015) 2116–2123, https://doi.org/10.1016/j.ceramint.2014.10.008.
[37] A. Metha, K. Khaoula, J. Kraxner, E. Hamada, G. Dušan, E. Bernardo, Upcycling of pharmaceutical glass into highly porous ceramics: from foams to membranes. Materials 15 (11) (2022) 3784, https://doi.org/10.3390/ma15113784.
[38] D. Lago, J. Kraxner, D. Galusek, E. Bernardo, Novel glass-based membranes for Cu adsorption: from alkali activation to sintering, e18221, Heliyon 9 (8) (2023), https://doi.org/10.1016/j.heliyon.2023.e18221.
[39] D. Lago, G. Tameni, F. Zorzi, J. Kraxner, D. Galuske, E. Bernardo, Novel cesium immobilization by alkali activation and cold consolidation of waste pharmaceutical glass, J. Clean. Prod. 461 (2024) 142673, https://doi.org/10.1016/j.jclepro.2024.142673.
[40] G. Barone, C. Finocchiaro, I. Lancellotti, C. Leonelli, P. Mazzoleni, C. Sgarlata, A. Stroscio, Potentially of the use of pyoclastic volcanic residues in the production of alkali activated material, Waste Biomass-.-. Valoriz. 12 (2021) 1075–1094, https://doi.org/10.1007/s12649-020-01004-6.
[41] M.F. Ashby, Chapter 1, Butterworth-Heinemann, Mater. Sel. Mech. Des. (2011) 1–13, https://doi.org/10.1016/B978-1-85617-663-7.00001-1.
[42] Y. Liu, C. Shi, Z. Zhang, N. Li, Conservation and Recycling, An overview on the reuse of waste glasses in alkali-activated materials, Resources 144 (2019) 297–309.
[43] A. Rincón, G. Giacomello, M. Pasetto, E. Bernardo, Novel ‘Inorganic Gel Casting’ process for the manufacturing of glass foams, J. Eur. Ceram. Soc., E. 37 (5) (2017) 2227–2234, https://doi.org/10.1016/j.jeurceramsoc.2017.01.012.
[44] A. Rincon Romero, S. Tamburini, G. Taveri, J. Toušek, I. Dlouhy, E. Bernardo, Extension of the ‘Inorganic Gel Casting’ process to the manufacturing of boro-alumino-silicate glass foams, Materials 11 (2018) 2545, https://doi.org/10.3390/ma11122545.
[45] G. Shao, X.Kong Wu, Y. Cui, X. Shen, C. Jiao, J. Jiao, Thermal shock behavior and infrared radiation property of integrative insulations consisting of MoSi2/borosilicate glass coating and fibrous ZrO2 ceramic substrate, Surf. Coat. Technol. 270 (2015) 154–163, https://doi.org/10.1016/j.surfcoat.2015.03.008.
[46] M.T. Carrasc, F. Puertas, Sodium silicate solutions from dissolution of glass wastes. Statistical analysis, e014, Mater. De. Construcion 64 (134) (2014), https://doi.org/10.3989/mc.2014.05213.
[47] M.A. Longhi, B. Walkley, E.D. Rodríguez, A.P. Kirchheim, Z. Zhang, H. Wang, New selective dissolution process to quantify reaction extent and product stability in metakaolin-based geopolymers, Compos. Part B: Eng. 176 (2019) 107172, https://doi.org/10.1016/j.compositesb.2019.107172.
[48] Y. Inagaki, T. Kikunaga, K. Idemitsu, T. Arima, Initial dissolution rate of the international simple glass as a function of the pH and temperature measured using microchannel flow-through test method, Int. J. Appl. Glass Sci. 4 (4) (2013) 317–327, https://doi.org/10.1111/ijag.12043.

[49] H.A. Elbatal, M.A. Azooz, E.A. Saad, F.M. Ezzeldin, M.S. Amin, Corrosion behavior mechanism of borosilicate glasses towards different leaching solutions evaluated by the grain method and FTIR spectral analysis before and after gamma irradiation, Silicon 10 (2018) 1139–1149, https://doi.org/10.1007/s12633-017-9586-1.
[50] N. Dogan-Saglamtimur, Waste foundry sand usage for building material production: a first geopolymer record in material reuse, Adv. Civ. Eng. 2018 (2018) 1927135, https://doi.org/10.1155/2018/1927135.
[51] R. Siddique, Y. Aggarwal, P. Aggarwal, E.-H. Kadri, Strength, durability, and micro-structural properties of concrete made with used-foundry sand (UFS) (Bennacer, R.), Const. Build. Mater. 25 (4) (2011) 1916–1925.
[52] Khatib, J.M.; Baig, S.; Bougara, A.; Booth, C., 2nd International Conference on Sustainable Construction Materials and Technologies, 2010, 931-935.
[53] C. Sgarlata, M.C. Ariza-Tarazona, E. Paradisi, C. Siligardi, I. Lancellotti, Use of foundry sands in the production of ceramic and geopolymers for sustainable construction materials, Appl. Sci. 13 (8) (2023) 5166, https://doi.org/10.3390/app13085166.
[54] S.T. Ferrazzo, M.T.D. Araujo, G.J. Bruschi, H. Mansur Chaves, E.P. Korf, N.C. Consoli, Mechanical and environmental behavior of waste foundry sand stabilized with alkali-activated sugar cane bagasse ash-eggshell lime binder, Const. Build. Mater. 282 (2023) 131313, https://doi.org/10.1016/j.conbuildmat.2023.131313.
[55] S. Apithanyasai, N. Supakata, S. Papong, The potential of industrial waste: using foundry sand with fly ash and electric arc furnace slag for geopolymer brick production, e03697, Heliyon 6 (3) (2020), https://doi.org/10.1016/j.heliyon.2020.e03697.
[56] V.M. Malhotra, Making concrete 'greener' with fly ash, 61-22, Acids Concr. Int. 12 (1999), https://doi.org/10.3390/ma15062050.
[57] R. Irizarry, A. Nararaj, J. Schoell, CLD-to-PSD model to predict bimodal distributions and changes in modality and change in modality and particle morphology. J. Chem. Eng. 232 (2021) 116332 https://doi.org/10.1016/j.ces.2020.116332.
[58] S. Fiore, M.C. Zanetti, Foundry wastes reuse and recycling in concrete production, Am. J. Environ. Sci. 3 (3) (2007) 135–142, https://doi.org/10.3844/ajessp.2007.135.142.
[59] Z. Gong, L. Liao, G. Lv, X. Wang, A simple method for physical purification of bentonite, Appl. Clay Sci. 119 (2)) (2016) 294–300, https://doi.org/10.1016/j.clay.2015.10.031.
[60] Y. Qin, T. Peng, H. Sun, L. Zeng, Y. Li, C. Zhou, Effect of montmorillonite layer charge on the thermal stability of bentonite, Clays Clay Min. 269 (2021) 328–338, https://doi.org/10.1007/s42860-021-00117-w.
[61] A.S. Zavertkin, Use of quartz and quartz-feldspar sands in molding mixes for casting iron, Refract. Ind. Ceram. 54 (2014) 438–442, https://doi.org/10.1007/s11148-014-9629-8.
[62] L.M. Costa, N.G.S. Almeida, M. Houmard, P.R. Cetlin, G.J.B. Silva, M.T.P. Aguilar, Influence of the addition of amorphous and crystalline silica on the structural properties of metakaolin-based geopolymers, Appl. Clay Sci. 215 (2021) 106312, https://doi.org/10.1016/j.clay.2021.106312.
[63] A.A.M. Ismail, K. Kannadasan, P. Pichaimani, H. Arumugam, A. Muthukaruppan, Synthesis and characterization of sodium silicate from spent foundry sand: effective route for waste utilisation, J. Clean. Prod. 264 (2020) 121689, https://doi.org/10.1016/j.jclepro.2020.121689.
[64] M.U. Okoronkwo, S.K. Mondal, B. Wang, H. Ma, A. Kumar, Formation and stability of gismondine-type zeolite in cementitious systems, J. Am. Ceram. Soc. 104 (2021) 1513–1525, https://doi.org/10.1111/jace.17572.
[65] El-Eswed, B.I , Alkali-Activated Materials in Environmental Technology Applications. Solidification/stabilization of hazardous wastes by alkali activation, 2022, Woodhead Publishing, Kidlington (UK), pp. 279-305, https://doi.org/10.1016/B978-0-323-88438-9.00011-9.
[66] P.R. Monich, A.R. Romero, D. Hollen, E. Bernardo, Porous glass-ceramics from alkali activation and sinter-crystallization of mixtures of waste glass and residues from plasma processing of municipal solid waste, J. Clean. Prod. 188 (2018) 871–878, https://doi.org/10.1016/j.jclepro.2018.03.167.
[67] Standard UNI EN 12457-2:2002. Characterisation of Waste—Leaching—Compliance Test for Leaching of Granular Waste Materials and Sludges—Part 2: One Stage Batch Test at a Liquid to Solid Ratio of 10 L/kg for Materials with Particle Size Below 4 mm (Without or With Size Reduction). Available online: https://standards.iteh.ai/catalog/standards/cen/db6fbdf3-1de7-457c-a506-46c4898e3f09/en-12457-2-2002 (accessed on 18.03.2024).
[68] F. Cioli, A. Abbà, C. Alias, S. Sorlini, Reuse or disposal of waste foundry sand: an insight into environmental aspects, Appl. Sci. 12 (13) (2022) 6420, https://doi.org/10.3390/app12136420.
[69] European Court of Auditors , EU actions to address the increasing amount of hazardous waste, Publications Office of the European Union, 2023, ⟨https://data.europa.eu/doi/10.2865/519218⟩.